Rotational Diffusion of Tracer Spheres in Packings and Dispersions of Colloidal Spheres Studied with Time-Resolved Phosphorescence Anisotropy

Minne Paul Lettinga,[†,‡] Carlos M. van Kats,[‡] and Albert P. Philipse*[,‡]

Section of Molecular Biophysics, Debye Research Institute, University Utrecht, Buys Ballot Laboratory, Princetonplein 5, 3584 CC, Utrecht, The Netherlands, and Van't Hoff Laboratory for Physical and Colloid Chemistry, Debye Research Institute, University Utrecht, Padualaan 8, 3584 CH, Utrecht, The Netherlands

Received December 9, 1999. In Final Form: March 31, 2000

We introduce the time-resolved phosphorescence anisotropy (TPA) method to study rotational diffusion of phosphorescent colloidal silica spheres in dispersions and in random close packings of host spheres. The tracer diffusion coefficients in sphere dispersions agree with hard-sphere predictions, demonstrating that TPA is a reliable technique for studying rotational dynamics. We also assess the rotational diffusion of phosphorescent tracers in sphere packings, exploiting the fact that the TPA technique can be used for slightly turbid samples. We find that the fraction of immobilized tracers directly reflects the pore size distribution as extracted from the Voronoi construction of a simulated random close packing. A calculation of the average distance between tracer and neighboring particle shows that the dependence of the rotational diffusion coefficient on the average distance between tracer and medium spheres is stronger for packings than for dispersions.

1. Introduction

The mobility of a colloidal particle in a confining geometry is predominantly determined by three factors, namely the geometrical constraints due to the matrix, hydrodynamic interactions between tracer and matrix, and any potential interactions between the matrix and the particle, e.g., van der Waals forces and Coulombic interactions. Studies on particles in confining geometries usually consider long-time translational diffusion, where particles move over distances many times their own size and consequently have many encounters within the confining medium. Examples of phenomenological approaches to study this translational diffusion are peak broadening in chromatography[1] and diffusion across membranes driven by a concentration gradient.[2] In situ determination of translational long-time self-diffusion coefficients has been performed by dynamic light scattering (DLS) studies on silica spheres in (cross-linked) polymer systems.[3,4] Another suitable method to study translational long-time self-diffusion is fluorescence recovery after photobleaching (FRAP). This method has been used, for example, to study diffusion of macromolecules through dextran methacrylate gels[5] and the mobility of membrane proteins inside the cell.[6]

Interpretation of long-time self-diffusion coefficients is complicated because geometrical constraints are often ill-defined and, moreover, little is known about the medium−tracer interactions. Several theories have been reported to tackle the problem.[7−10] An experimental approach to facilitate the interpretation of long-time self-diffusion experiments in complex media is to make use of model systems where specific interactions between tracer and host matrix can be controlled. This approach was followed by Kluijtmans et al.,[11−14] who used DLS and FRAP to determine translational long-time self-diffusion of spherical silica particles in porous glasses[12] and random sphere packings (rcp),[13] varying pore size and ionic strength.[14] These model systems offer several advantages. Surface properties of the host medium and tracer are well-defined, as well as the size of tracer particles. Moreover, the systems are stable in the sense that sticking between tracer and matrix is avoided. In the case of random sphere packings simulation results[15] and approximate models[7] were used to account for the influence of the geometry and hydrodynamics on the long-time self-diffusion behavior.[12]

Up till now most studies on diffusion in complex media have been focused on (long-time) translational diffusion. However, knowledge of the *rotational* diffusion coefficient D_r of the tracer will reveal different information on the interaction between host medium and tracer than knowledge of the translational diffusion coefficient D_L. One important difference between D_r and D_L measurements is that the structure of the host medium is probed on different spatial scales.[16,17] In random close packings, for example, D_L vanishes when the ratio β_{tr} of tracer radius

* Corresponding author.
† Section of Molecular Biophysics.
‡ Van't Hoff Laboratory for Physical and Colloid Chemistry.

(1) Hejtmanek, V.; Schneider, P. *Chem. Eng. Sci.* **1994**, *49*, 2575.
(2) Malone, D. M.; Anderson, J. L. *Chem. Eng. Sci.* **1978**, *33*, 1429.
(3) Phillies, G. D. J.; Clominel, D. *Macromolecules* **1993**, *26*, 167.
(4) Joosten, J. G. H.; Geladé, E. T. F.; Pusey, P. N. *Phys. Rev. A* **1990**, *42*, 2161.
(5) De Smedt, S. C.; Meyvis, T. K. L.; Demeester, J.; van Oosteveldt, P.; Blonk, J. C. G.; Hennink, W. E. *Macromolecules* **1997**, *30*, 4863.
(6) Storrie, B.; Kreis, T. E. *Trends Cell Biol.* **1996**, *6*, 321.
(7) Kim, I. C.; Torquato, S. *J. Chem. Phys.* **1992**, *96*, 1499.
(8) Ogston, A. G. *Trans. Faraday Soc.* **1958**, *54*, 1754.
(9) Tong, J.; Anderson, J. L. *Biophys. J.* **1996**, *70*, 1505.
(10) Ogston, A. G.; Preston, B. N.; Wells, J. D. *Proc. R. Soc. London* **1973**, *333*, 297.
(11) Kluijtmans, S. G. J. M. Dynamics of colloids in porous media. Thesis Utrecht University, The Netherlands, 1998.
(12) Kluijtmans, S. G. J. M.; Dhont, J. K. G.; Philipse, A. P. *Langmuir* **1997**, *13*, 4976.
(13) Kluijtmans, S. G. J. M.; Philipse, A. P. *Langmuir* **1999**, *15*, 1896.
(14) Kluijtmans, S. G. J. M.; de Hoog, E. H. A.; Philipse, A. P. *J. Chem. Phys.* **1998**, *108*, 7469.
(15) Pagonabarraga, I.; Hagen, M. H. J.; Lowe, C. P.; Frenkel, D. *Phys. Ref. E* **1999**, *59*, 4458.
(16) Jamil, T.; Russo, P. S. *Langmuir* **1998**, *14*, 264.
(17) Lavalette, D.; Tétreau, C.; Tourbez, M.; Blouquit, Y. *Biophys. J.* **1999**, *76*, 2744.

10.1021/la991603v CCC: $19.00
Published on Web 06/23/2000

R_{tr} to the sphere radius R_{pack} is larger than $\beta_{tr} \approx 0.15$, since the tracer cannot escape from the interstitial holes.[13] D_r, in contrast, is expected to vanish at much higher β_{tr}, because the confinement of a tracer to an interstitial space does not prohibit rotational tracer diffusion. The study of rotational diffusion of tracers in random packings of host spheres therefore provides information on the local structure. Furthermore, the interactions between tracers and host spheres can be studied when they come in close contact.

Rotational diffusion of spherelike particles is, however, difficult to access because the mechanical isotropic tracers need to have some kind of internal anisotropy for the detection technique used. Recently we synthesized phosphorescent silica spheres that, in combination with the time-resolved phosphorescence anisotropy technique (TPA), can be used to determine the rotational diffusion of silica particles.[18] The aim of this article is to apply TPA to study the mobility of these newly synthesized tracers in random packings of host spheres. By varying the size of the host spheres, we indeed are able to gain information on the local structure of a rcp and on the interactions between tracers and host spheres when they come in close contact.

The structure of packed host spheres is static, provided the host spheres are large enough for their Brownian motion to be negligible. We also studied the rotational dynamics for a thermally fluctuating confinement, i.e., for a colloidal dispersion with Brownian particles as host spheres. Here we used a series of sphere dispersions at a fixed value of β_{tr} (=0.95). This allows a comparison with measurements and theory as described by Degiorgio et al.[19] They used depolarized dynamic light scattering (DDLS) to study the rotational diffusion of optically anisotropic spheres in colloidal dispersions.

This paper is organized as follows. In section 2 we discuss how TPA can be applied to rotational diffusion measurements on colloidal systems. Section 3 briefly describes the sample preparation, the TPA technique, and the analysis of the TPA decay curves. In the discussion in section 4 we pay special attention to the influence of the microstructure of the rcp on the rotational and translational diffusion. For this purpose we used the Voronoi construction to analyze the structure of simulated rcp. Section 5 summarizes the main conclusions.

2. Time-Resolved Phosphorescence Anisotropy for Tagged Colloidal Spheres

In a time-resolved phosphorescence anisotropy experiment the sample is illuminated with a short vertically (V) polarized light pulse. The horizontal (H) or vertical (V) component of the emitted light is detected in a standard 90° geometry. The phosphorescence anisotropy $r_P(t)$ is then defined by

$$r_P(t) = \frac{I_{VV}(t) - I_{VH}(t)}{I_{VV}(t) + 2I_{VH}(t)} \tag{1}$$

If the sample is macroscopically isotropic, the anisotropy can be expressed as a single correlation function:[20]

$$r(t) = 2\langle D^{2*}_{00}(\Omega^t_{Lv})\, D^2_{00}(\Omega^0_{L\mu})\rangle \tag{2}$$

where D^L_{mn} is the Wigner rotation matrix of angle Ω. $\Omega^0_{L\mu}$ and Ω^t_{Lv} represent the orientations of the absorption dipole moment $\vec{\mu}$ at $t = 0$ and emission dipole moment $\vec{\nu}$ at time t relative to the director of the laboratory frame L. $\Omega_{L,\mu,\nu}$ can be separated into three sequential orientations: the orientation Ω_{Ld} of the local director of the tracer d in the laboratory frame L, the orientation Ω_{dl} of the long axis of the dye l relative to the local director d, and the orientation of the absorption and emission dipole moments $\vec{\mu}$ and $\vec{\nu}$ relative to the long axis of the dye l. Here we exploit the orthonormality of Wigner rotation matrices by using the closure relation.[21] The internal rotation of the dye relative to the local director of the tracer can be separated from the overall tumbling of the tracer if the difference between the two rotations is orders of magnitude. Furthermore, the problem can be simplified, considering the locally uniaxial distribution in the sphere and the uniaxial symmetry of the tracers themselves. With these consideration, (2) yields

$$r^{rot}_P(t) = \frac{2}{5}\langle D^2_{00}(\Omega^t_{Ld})\, D^2_{00}(\Omega^0_{Ld})\rangle \times \left[\sum_{m=-2,0,2} \langle D^2_{0m}(\Omega_{dl})\rangle D^2_{m0}(\Omega_\mu) \sum_{n=-2,0,2} \langle {D_{0n}}^2(\Omega_{dl})\rangle D^2_{n0}(\Omega_\nu)\right] \tag{3}$$

The term within the square brackets gives the correlation function of the local reorientation of the dye molecules. The value of this term can be determined in separate experiments.[18,22]

The first term gives the rotational diffusion correlation function of the tracer particles, which is the function relevant in the present study. In the case of monodisperse and noninteracting spheres, this correlation function can be described by a single exponential

$$\langle D^2_{00}(\Omega^t_{Ld})\, D^2_{00}(\Omega^0_{Ld})\rangle = \exp(-6D^r_0 t) \tag{4}$$

where D^r_0 is the rotational diffusion coefficient at infinite dilution. D^r_0 is given by the Stokes−Einstein relation for rotating spheres, which depends on volume V of the rotating sphere, temperature T, and viscosity η of the solvent:

$$6D^r_0 = \frac{k_B T}{\eta V} \tag{5}$$

However, here we are dealing with the rotational diffusion of tracer particles with a polydispersity of about 10% in a dense packing of host spheres. Because of the polydispersity of the tracers and the expected variation of the local microviscosity throughout the packing, for such a system a distribution of diffusion coefficients D^r_i should be considered in the analysis. Therefore, data were analyzed using a multiexponential as a model for the anisotropy decay $r_P(t)$:

$$r_P(t) = r_P(t_d)\sum_i a_i \exp(-6D^r_i t) \tag{6}$$

where a_i is the contribution of the diffusion coefficient D^r_i and $r_P(t_d)$ is the effective initial anisotropy as determined in earlier experiments.[18]

(18) Lettinga, M. P.; van Zandvoort, M. A. M. J.; van Kats, C. M.; Philipse, A. P. *Langmuir* **2000**, *76*, preceding paper in this issue.
(19) Degiorgio, V.; Piazza, R.; Jones, R. B. *Phys. Rev. E* **1995**, *52*, 2707.
(20) Zannoni, C. In *The molecular Physics of Liquids*; Luckurst, G. R., Gray, G. W., Eds.; Academic Press: London, 1979.
(21) Rose, M. E. *Elementary theory of angular momentum*; Wiley: New York, 1957.
(22) Lettinga, M. P. Phosphorescence spectroscopy and its application to the study of colloid dynamics. Thesis, Utrecht University, The Netherlands, 1999.

Table 1. Characteristics of Host and Tracer Spheres

packing particle	R_{TEM} (nm)	σ^a	β_{tr} (=113/R_{TEM})
SC_{06}	123	0.06	0.862
S163	163	0.04	0.650
SC_{07}	204	0.02	0.520
SC_{08}	270	0.02	0.393
SB284	284	0.05	0.373
VIII	347	0.04	0.305
SC01	392	0.03	0.270
SC03	458	0.02	0.231
SC04	622	0.02	0.170
SC06	828	0.02	0.128
AS30	1675	0.13	0.063
tracers	**R_{TEM} (nm)**	**σ^a**	**R_{TPA}**
P113	113	0.10	131 ± 3
P117	117	0.10	132 ± 5

[a] Size polydispersity.

The possibility to extract different exponents from the data analysis is limited.[23] As an example, we consider two limiting cases. First, suppose there are two diffusion coefficients: $D_1^r = 0.8D_2^r$ and $a_1 = a_2$. Simulations show that for this case the decay curve is equally well fit by a monoexponential as by a biexponential. Thus, the polydispersity of the tracer particles of 10% does not lead to a clearly detectable multiexponential decay. If, on the other hand, D_2^r is much lower than D_1^r and $1/D_1^r$ is on the order of the phosphorescence lifetime, then the best fit is often a single decay component with a plateau ($D_2^r = 0$). This limiting case is reached around $D_2^r = 0.1D_1^r$. Note that spherical particles by definition do not have an overall orientational axis. Therefore, a plateau in the anisotropy decay does not point to ordering of an orientational axis, but to the presence of a very slow decay component.

3. Experimental Section

3.1. Preparation and Characterization of the Medium Particles. To have a sufficiently wide range in values of $\beta_{tr} = R_{tr}/R_{pack}$, a fairly large number of silica systems is needed. Sphere packings were prepared from silica spheres of various sizes, some of which were used earlier by Kluijtmans et al.[13] Information on these silica spheres is summarized in Table 1. Particle sizes were determined with transmission electron microscopy (TEM) using a Philips CM10H electron microscope. Particle size distributions were obtained by determining the size of about 100 separate particles. The polydispersity is defined as the standard deviation of the distribution divided by the mean particle radius.

The particles coded SC were made by a seeded growth procedure following the method of Giesche.[24,25] Silica seeds (R_{TEM} = 202 nm) were prepared by the Stöber method.[26] The particles were grown by continuously adding two feed solutions in equal amounts at a rate of 10 mL/h under continuous stirring to 80 mL starting dispersion of silica seeds (0.65 M) in ethanol, containing ammonium hydroxide (0.5 M, Merck) and H_2O (10 M). The first solution was ammonium hydroxide (1.12 M) and H_2O (16 M) in ethanol. The second solution was 2 M TES in ethanol. Samples were taken from the reaction vessel twice a day for 5 days and coded in chronological order. After 2 days the start of a second silica nucleation was observed. These secondary particles were separated by repeated centrifugation and coded with the serial number as a subscript. All SC particles were transferred to a solution of *N*,*N*′-dimethylformamide (DMF, Sigma-Aldrich) by repeated centrifugation and redispersion. SB284 and S163 were synthesized separately.

Silica AS30 was obtained as powder from Alltech (Deerfield, IL). The material, which is used as column packing, is readily redispersable. TEM showed no clustering or large aggregates. Its particle size polydispersity of 13%, however, is substantial. The synthesis and characterization of the VIII particles is described by Kluijtmans.[13] The phosphorescent colloidal silicas P113 and P117 were used as optical tracers. The synthesis and characterization of the tracer particles P113 and P117 are described elsewhere.[18]

TPA measurements on tracer particles in a dense packing or dispersions of spheres require optically matching of the porous medium. Therefore host spheres were transferred to a mixture of DMF and dimethyl sulfoxide (DMSO) (40:60 v/v) with a refractive index of 1.46. The salt concentration was fixed at 0.01 M LiCl. The volume fractions of the so-obtained stock dispersions (φ_{dry}) were determined by drying a known volume of the dispersion and dividing the weight of the solid residue by the silica mass density of 1.8 ± 0.1 g/mL. This density has been reported for various silica colloids.[27]

3.2. Preparation of Sphere Packings and Dispersions. A series of dispersions was prepared from a sediment of SC_{06} (R_{TEM} = 123 nm) with a volume fraction $\varphi_{dry} = 0.46$ in a mixture of DMF and DMSO (40:60) 10 mM LiCl. We used P117 as a tracer (R_{TEM} = 117 nm). The tracer concentration was 0.12% v/v for all dispersions. For the effective volume fraction of the sediment we have to consider that the particles may have a solvation layer of solvent molecules.[28,29] The radius of the dry particles R_{dry} can be found, assuming that the shrinkage of the particles due to radiation damage of the electron beam is 5%.[28] R_{dry} = 123 nm for the tracer P117, which is 10 nm smaller than the hydrodynamic radius R_{DLS}. The solvation layer of 10 nm is comparable to the value found by Imhof and Dhont for pure DMF.[29] The effective volume fraction is now $\varphi_{eff} = (132/123)^3 \cdot (0.46) = 0.57$.

The sphere packings were prepared as follows. In a small glass vial (100 × 4 × 0.4 mm, Vitro Dynamics) 50 μL of a concentrated dispersion of host spheres (ca. 20% v/v) and phosphorescent tracers P113 (between 0.7% and 3% v/v, increasing with R_{pack}) was centrifuged. The centrifugation time was chosen between 5 min at 2000 rpm for AS30 and 40 min at 3000 rpm for SC_{06}. Following this procedure we took care that the final tracer concentration in the packing was approximately the same for all packings. The samples were used the same day for the TPA experiment. The volume fraction of the packings was determined by preparing a packing with a dispersion of known volume fraction and measuring the height of sediment relative to the total height of the fluid in the vial. A few dried packings were inspected with scanning electron microscopy (SEM, Philips, XL30FEG at 10 kV).

3.3. TPA Measurements and Analysis. The time-resolved phosphorescence setup is described in detail in refs 22 and 30. Here we summarize the essential features of the setup. A vertically polarized excitation source (Nd:YAG laser 10 Hz (Continuum)) was used to excite the sample at 532 nm. The vial with the sample was placed at an angle of 45° with the incident beam in a cuvette containing toluene for optical matching. The emission light was detected under 90° with the excitation beam. A sheet polarizer was used to select the polarization direction of the emission light. In this way two signals were captured: $I_{VV}(t)$ for the vertically polarized emission light and $I_{VH}(t)$ for the horizontally polarized emission light. The anisotropy is calculated from these two signals (see (1)).

The numerical analysis of the time-resolved experimental data was carried out using the ZXSSQ routine from the IMSL program library to fit the data to the model of choice (see (6)) with the nonlinear least-squares method of Levenberg and Marquardt. The experimental decay curves from the time-resolved experiment were analyzed using a reiterative nonlinear least-squares deconvolution technique.[31]

(23) van der Sijs, D. A.; van Faassen, E. E.; Levine, Y. K. *Chem. Phys. Lett.* **1993**, *216*, 559.
(24) Giesche, H. *J. Eur. Ceram. Soc.* **1994**, *14*, 189.
(25) Giesche, H. *J. Eur. Ceram. Soc.* **1994**, *14*, 205.
(26) Stöber, W.; Fink, A.; Bohn, E. *J. Colloid Interface Sci.* **1968**, *26*, 62.
(27) Philipse, A. P.; Pathamanoharan, C. *J. Colloid Interface Sci.* **1993**, *159*, 96.
(28) van Helden, A. K.; Jansen, J. W.; Vrij, A. *J. Colloid Interface Sci.* **1981**, *81*, 354.
(29) Imhof, A.; Dhont, J. K. G. *Phys. Rev. E* **1995**, *52*, 6344.
(30) Lettinga, M. P.; Klarenbeek, E. M.; Zuilhof, H.; van Zandvoort, M. A. M. J. *J. Fluoresc.* **1999**, *9* (3), 265.

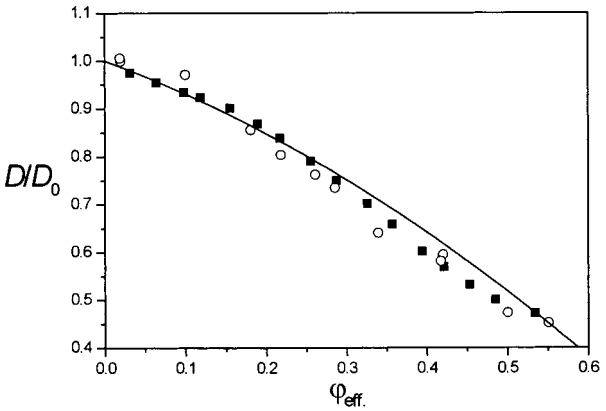

Figure 1. Reduced rotational diffusion coefficient of phosphorescent silica tracers (P117) in a dispersion of SC_{06} host spheres ($\beta_{tr} = 0.95$) as a function of the volume fraction φ_{eff} of host particles (○), compared with the data of Degiorio et al.[19] (■). The drawn line is the theoretical prediction for hard spheres with hydrodynamic interactions.[19]

4. Results and Discussion

4.1. Rotational Diffusion in Sphere Dispersion. We have measured the rotational diffusion of P117 (R_{TEM} = 117 nm) in a SC_{06} dispersion (R_{TEM} = 123 nm) as a function of the volume fraction of host spheres in a mixture of DMF and DMSO (40:60) 10 mM LiCl. The TPA data were fitted using a monoexponential decay. In Figure 1 the reduced diffusion coefficient (D/D_0) is plotted as a function of the effective volume fraction. Our results agree with the experimental and theoretical results of Degiorgio et al.[19] The latter authors used DDLS to measure the rotational diffusion in dispersions of 110 nm optically anisotropic spheres and compared their results with theoretical calculations (including hydrodynamic interactions) on the short-time rotational diffusion of hard spheres. Our results confirm that TPA is a reliable technique for the determination of rotational diffusion coefficients of colloidal silica spheres and that the tracers as characterized in ref 18 behave as hard spheres. Thus, we are able to access the rotational diffusion of phosphorescent spherical tracers in confining media.

4.2. Characterization of the Tracers and the Sphere Packings. The tracer concentration in the sphere packings was estimated comparing the phosphorescence intensity detected from the packings with the phosphorescence intensity detected from a solution with a known tracer concentration. For most values of β_{tr} ($=R_{tr}/R_{pack}$), tracer concentrations in the packing were typically 0.1% v/v, starting with concentrations of ca. 0.3% v/v in the dispersion before centrifugation. A sediment of tracer particles was formed on top of the packing for these samples. At higher values of β_{tr} (>0.5) the tracer concentration in the packing increased, while smaller sediments of tracer particles were observed on top of the packings.

The sphere packings were transparent for host spheres SC_{06} to VIII (Table 1). For larger host spheres, packings had a slightly opaque homogeneous appearance, nevertheless they were sufficiently optically matched for TPA measurements. In none of the packings visible Bragg reflections were observed, which suggests that the host spheres were randomly packed. This is confirmed by the SEM micrographs in Figure 2 and similar micrographs made by Kluijtmans.[13] The random sphere packings have

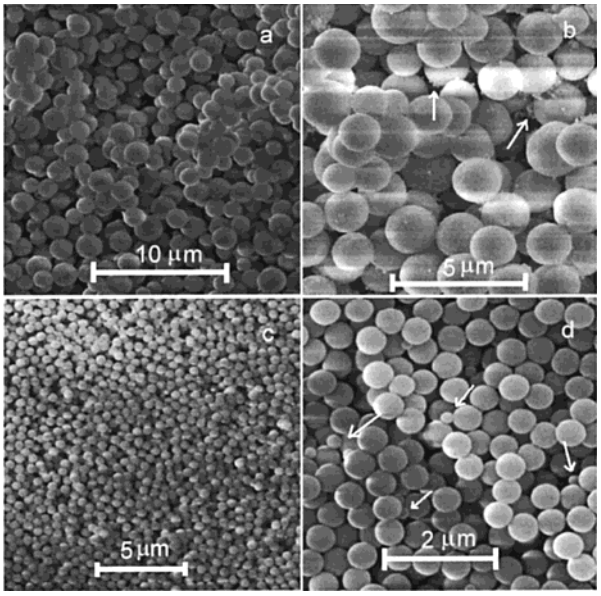

Figure 2. Scanning electron micrographs of a cross section of a dried packing with AS30 (upper graphs) and SC_{08} (bottom graphs) spheres, containing the tracer P113. The graphs on the left give an overview of the cross-section area. Arrows at the right point to tracer particles present in the sample. Due to the capillary forces when the sample is dried, the tracers accumulate in the narrow inclusions between touching AS30 spheres (b). For SC_{08} there is no accumulation due to the small pore sizes (c).

a volume fraction in the range of 65% ± 5%, which is comparable to the random close packing value of 64%. Our packing density range is comparable to other values found for silica sphere packings.[27]

For the optically clear packings of SC_{06} to VIII and AS30, we found an effective initial anisotropy of 0.12. However, for the particles SC01 to SC04 the effective initial anisotropy decreased to 0.09. This decrease is probably due to depolarization effects caused by scattering of the packing. This effect does not hinder the analysis of the anisotropy decays.

4.3. Rotational Diffusion in Sphere Packings. Typical TPA curves are shown in Figure 3, where the TPA is given for four values of the size ratio β_{tr}. For small values of β_{tr} (up to β_{tr} = 0.178) the phosphorescence anisotropy decays were best fitted with a double exponential decay. The typical slow decay time component for these fits was 5−9 times the phosphorescence lifetime, i.e., between 15 and 27 ms. For higher values of β_{tr} the curves were best fitted using a monoexponential decay with a plateau. The level of this plateau indicates the fraction of tracer molecules that are immobilized on the phosphorescence time scale, i.e., which have a decay time of around 30 ms or higher. Note that this limitation in dynamic range can be circumvented when polarized fluorescence recovery after photobleaching is applied, following the scheme of Cicerone and Ediger, who used this technique to study the rotational diffusion of small molecules at the glass transition.[32] The same tracer may be use for this purpose, since eosin is known for its bleachability.

The reduced diffusion coefficient and the fraction of immobilized tracers are plotted in Figure 4 as a function of β_{tr}. Because the differences in quality, expressed by χ^2, between the double exponential fit and the monoexponential fit with plateau were marginal for $\beta_{tr} < 0.178$, we

(31) Cundall, R. B.; Dale, R. E. *Time-resolved Fluorescence Spectroscopy in Biochemistry and Biology*; Plenum Press: New York, 1983.

(32) Cicerone, M. E.; Ediger, M. D. *J. Phys. Chem.* **1993**, *97*, 10489.

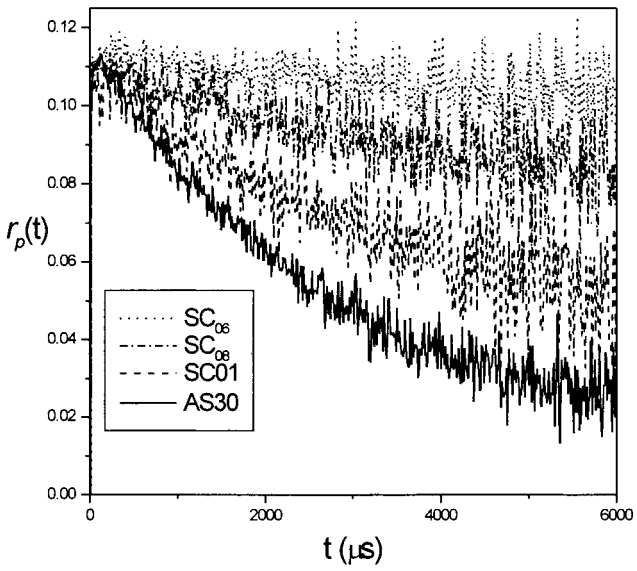

Figure 3. TPA decay curves showing the rotational diffusion of eosin-labeled tracers with a TEM radius of 113 nm in four different packings of host spheres. The radius of the host spheres is varied between 1675 and 213 nm (see Table 1).

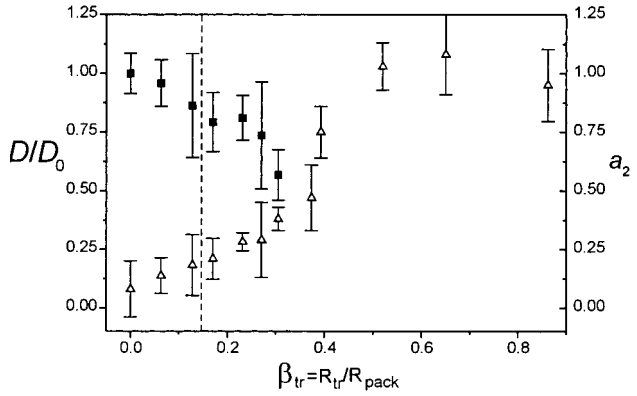

Figure 4. Reduced rotational diffusion coefficient D/D_0 (■) and contribution of immobilized tracers a_2 (△) as a function of β_{tr}. The values are obtained from a monoexponential fit with a plateau a_2 of the TPA decay curves. The dashed line marks the point after which translational diffusion is prohibited ($\beta_{tr} \approx 0.15$).[13]

used the results of the monoexponential fit plus plateau for all values of β_{tr}. Each point is an average of four to eight measurements, and the error margins are given by the standard deviation. The values for $\beta_{tr} = 0$ represent the rotational diffusion of P113 in solution. In the ideal case the value for a_2 is zero. Here we find however a value of 0.08 ± 0.13. This deviation may indicate that there were some aggregates in the sample. For $\beta_{tr} > 0.4$ it is virtually impossible to accurately determine the reduced diffusion coefficient because of the very small population of freely rotating particles.

4.4. Pore Size Distribution in Random Close Packing (rcp): Voronoi Construction. For the interpretation of the rotational diffusion in sphere packings, a theoretical model is needed describing the effect of hydrodynamic interactions on the rotational diffusion of a spherical tracer in a confined space. In addition, information on the microstructure of the random close packing of spheres has to be implemented in the analysis.

For long-time translational self-diffusion measurements a suitable reference model is the translational diffusion of a sphere in a capillary or slit[13] for which the hydrodynamic effects can be calculated.[33] For rotation in a static medium to our knowledge only one reference is available by Philips et al.,[34] who performed Monte Carlo simulations on suspensions of both immobilized and free hard spheres using Stokesian dynamics to calculate the rotational diffusion of a free tracer sphere. Their work, nevertheless, does not apply to our measurements in a straightforward way, since the immobilized spheres do not constitute a rcp and there is no tracer sphere of a smaller size probing the available free space. However, their results may be used for a qualitative comparison considering the influence of a static environment and a fluctuating environment on the rotational diffusion coefficients; see section 4.5.

We note that there are several references where the influence of the volume fraction of hard-sphere dispersions on the rotational diffusion is calculated[19,35] or simulated.[36] Jones and Alavi[37] did calculate the influence of a single hard wall potential on the rotational diffusion, but this geometry does not reflect the physical situation of a tracer in a rcp. Calculations for a rotational diffusion model in Brinkman fluids have also been reported.[38] It has been shown, however, that the Brinkman approach does not correctly describe the hydrodynamic permeability at high densities near or close to rcp.[27] Though theory on the influence of hydrodynamic interactions on rotational diffusion in confined media is not available yet, we do have reliable information on the relative coordinates of spheres in a rcp.[39] Kluijtmans et al.[13] used the coordinates of the rcp to calculate the conductivity of silica sphere packings. However, this conductivity is not relevant here, since it is defined as the change in the *translational* diffusion due to geometrical constraints of the matrix. We expect that rotational diffusion is rather determined by the distribution of shortest distances between tracer and host spheres. Since we have shown that host and tracer particles behave as the hard spheres (Figure 1), it seems plausible that during the sedimentation of tracer−host mixtures the tracer particles are pushed toward the nearest available free volume. This free volume can be estimated from the distance between the center point of the tracer sphere and the surface of the nearest host sphere. If the real-space structure of the sphere packing is known, then the center points can be found in a unique way through the Voronoi construction; see Figure 5.

A Voronoi polyhedron contains all the points in space that are closer to the center of the particle than to all other particles. All particles share a face of their Voronoi polyhedron with another particle. The vertices of the polyhedron are the points where three faces intersect. The shortest distance from a vertex to a sphere surface therefore is a measure of the available free space for a tracer. This typical distance will be called the pore size R_{pore}. The corresponding relative distance β_{pore} is defined as $\beta_{pore} = R_{pore}/R_{pack}$, where R_{pack} is the radius of the host spheres.

Here we perform an analysis on a computer-simulated rcp, using an adapted version of the program voron3d.[40] The resemblance between the real-space structure of the simulated rcp and an actual rcp of dye-labeled silica

(33) Anderson, J. L.; Quinn, J. A. *Biophys. J.* **1974**, *14*, 130.
(34) Philips, R. J.; Brady, J. F.; Bossis, G. *Phys. Fluids* **1988**, *31*, 3473.
(35) Watzlawek, M.; Nägele, G. *Physica A* **1997**, *235*, 56.
(36) Philips, R. J.; Brady, J. F.; Bossis, G. *Phys. Fluids* **1988**, *31*, 3462.
(37) Jones, R. B.; Alavi, F. N. *Physica A* **1992**, *187*, 436.
(38) Solomentsev, Y. E.; Anderson, J. L. *Phys. Fluids* **1996**, *8*, 1119.
(39) van Blaaderen, A.; Wiltzius, P. *Science* **1995**, *270*, 1177.
(40) Allen, M. P.; Tildesley, D. J. *Computer Simulations of Liquids*; Clarendon Press: Oxford, Great Britain, 1987.

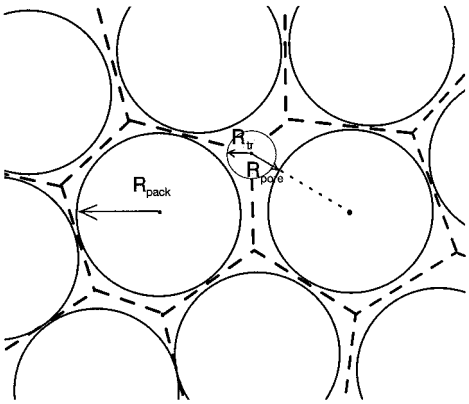

Figure 5. Illustration of the Voronoi construction of a random close packing in two dimensions. The edges of the Voronoi polyhedron, for which every point has an equal distance to two sphere centers, are given by the dashed lines. The gray sphere is a tracer particle.

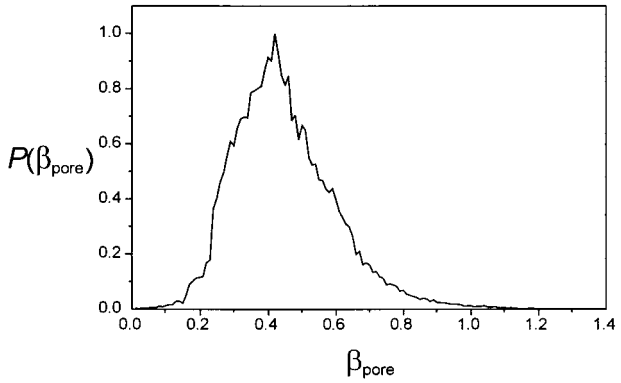

Figure 6. Pore size distribution $P(\beta_{pore})$ as obtained from a Voronoi construction of a simulated random close packing of spheres.

spheres was demonstrated elsewhere, using confocal fluorescence microscopy.[39] The pore size distribution $P(\beta_{pore})$ is given in Figure 6. For this figure 30 cubes were analyzed, each containing up to 95 spheres taken at random from the simulated rcp and calculated the Voronoi construction. In this way, up to 110 000 vertices were collected.

A simple method to estimate the amount of immobilized tracer particles in a rcp is to assume that the particles are immobilized when the distance between tracer and host particle is smaller than a certain distance ΔR. To find an estimate for the fraction of immobilized particles a_2 at a ratio β_{tr}, the integral over $P(\beta_{pore})$ from $\beta_{pore} = 0$ to $\beta_{tr} + \Delta\beta_{tr}$ (with $\Delta\beta_{tr} = \Delta R/R_{tr}$) has to be divided by the total integral taken from $\beta_{pore} = 0$ to β_{pore}^{max}, the highest value for β_{pore} found from the Voronoi construction:

$$a_2(\beta_{tr}) = \frac{1}{N}\int_0^{\beta_{tr}+\Delta\beta_{tr}} P(\beta_{pore})\, d\beta_{pore} \qquad (7)$$

with

$$N = \int_0^{\beta_{pore}^{max}} P(\beta_{pore})\, d\beta_{pore} \qquad (8)$$

The result of this model and a comparison with our experimental data are shown in Figure 7. We used a ratio of $\Delta R/R_{tr}$ between 0 and 0.3. The better fit from the four curves is given by $\Delta R = 0.2R_{tr}$. Taking for the tracer radius the hydrodynamic radius of 132 nm, this suggests that the rotational diffusion is at least 10 times reduced

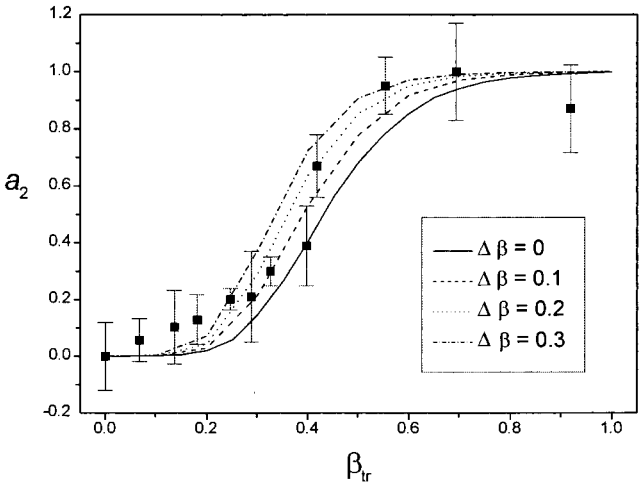

Figure 7. Fraction of immobilized tracer particles. Experimental values as compared to the values calculated using eq 9, for four threshold radii ΔR.

compared to D_0 when the distance between the surfaces of the tracer and the host spheres is less than 26 nm. It should be noted that the tracers are assumed to be homogeneously distributed over the packing, independent of the available free volume. In other words, for $R_{tr} \geq R_{pack}$ tracers particles are assumed not to have translated toward a larger neighboring pore. When tracer spheres are allowed to escape, the pore size distribution used in (7) should be adapted. This would probably result in a steeper curve and therefore in a smaller value for ΔR. Furthermore, the polydispersity of the tracers and host spheres was not taken into account. The deviations at large size ratios for which $\beta_{tr} < 0.2$ (see Figure 7) may indicate that tracer particles occasionally adsorb on packings of sufficiently large spheres when $R_{tr} \ll R_{pack}$. Such an adsorption effect has been reported earlier by Thies-Weesie et al.[41] for bidisperse mixtures of grafted silica spheres and small Ludox spheres. From the analysis of the fraction of immobilized tracers, we can conclude that the pore size distribution $P(\beta_{pore})$ found from the Voronoi construction of the computer simulated rcp models the microstructure of the rcp satisfactorily.

4.5. Comparison between Rotational Dynamics of Tracers in Random Sphere Packings and Dispersions. To compare the reduced rotational diffusion coefficients in a static (packing) environment and a fluctuating (dispersions) environment, our data should be rescaled, so that we can compare our experimental results with simulations performed by Phillips et al.[34,36] Instead of the effective volume fraction of the dispersion φ_{eff} and the ratio β_{tr} of the sphere packings, we now use the average reduced free distance $\langle\lambda\rangle$. In the case of sphere packings $\langle\lambda\rangle$ is the ratio of the tracer radius to the average pore size: $\langle\lambda_{pore}\rangle = R_{tr}/\langle R_{pore}\rangle = \langle\beta_{tr}/\beta_{pore}\rangle$. $\langle\lambda_{pore}\rangle$ is calculated by

$$\langle\lambda_{pore}(\beta_{tr})\rangle = \int_{\beta_{tr}+\Delta\beta_{tr}}^{\beta_{pore}^{max}} P(\beta_{pore})\frac{\beta_{tr}}{\beta_{pore}}\, d\beta_{pore} \Big/ \int_{\beta_{tr}+\Delta\beta_{tr}}^{\beta_{pore}^{max}} P(\beta_{pore})\, d\beta_{pore} \qquad (9)$$

where integration is taken over all mobile particles, i.e., $\beta_{pore} > \beta_{tr} + \Delta\beta_{tr}$.

For dispersions, $\langle\lambda\rangle$ is the ratio of the tracer radius to the average distance between the center of the tracer and

(41) Thies-Weesie, D. M. E.; Philipse, A. P.; Lekkerkerker, H. N. W. *J. Colloid Interface Sci.* **1996**, *171*, 438.

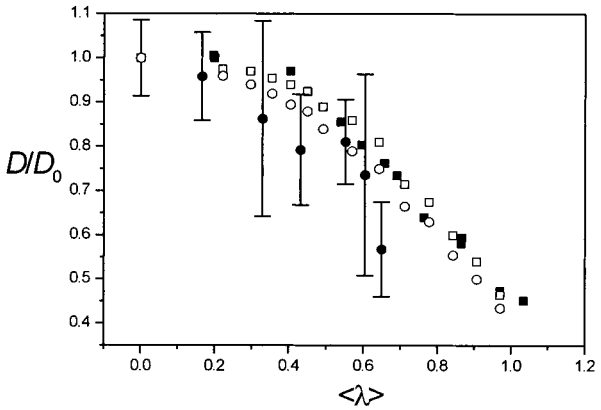

Figure 8. Reduced rotational diffusion coefficient as a function of the average reduced free volume $\langle\lambda\rangle$. The circles give the results for tracer diffusion in packings of immoblized host spheres. The cubes give the results for tracer diffusion in dispersions. The open symbols represent our TPA data, while the solid symbols represent the results of the simulations by Phillips et al.[34,36]

the surface of a medium sphere.

$$\langle\lambda_{\text{disp}}\rangle = \left[\left(\frac{4}{3}\pi\frac{1}{\varphi_{\text{eff}}}\right)^{1/3} - 1\right]^{-1} \tag{10}$$

The rescaled data are depicted in Figure 8 together with the results of Philips et al., who simulated the volume fraction dependence of the rotational diffusion of a tracer sphere in a suspension of mobile[36] and immobilized[34] medium spheres. Like Philips et al., we find that the rotational diffusion in a surrounding of immobilized spheres depends slightly stronger on the relative distance than in a surrounding of mobile spheres.

5. Conclusions

Time-resolved phosphorescence anisotropy measurements were used to study the rotational diffusion of phosphorescent spherical silica tracers in dispersions of different volume fractions and in static random packings of host spheres. The measurements on dispersions agree with theoretical predictions for hard spheres, demonstrating the suitability of the tracers as well as the TPA technique. We have shown that the fractions of immobilized tracers in sphere packings quite accurately mimic the pore size distribution resulting from a Voronoi analysis on a simulated random close packing. The reduced rotational diffusion coefficients for dispersions and packings showed the same qualitative dependency on the average reduced free distance as was found earlier by Monte Carlo simulations.[34]

Our rotational diffusion measurements of spherical tracers in a rcp confirm that rotational diffusion measurements are a more local probe of complex media than translational long-time self-diffusion.[13] The translational diffusion depends on the conductivity of the host medium, whereas rotational diffusion depends on the local pore sizes. As a result, tracer rotation may occur at pore sizes which would arrest long-time translational self-diffusion. Thus, by combining translational and rotational diffusion measurements, a distinction can be made between sterical entrapment by the host medium and immobilization due to attractions between tracer and host medium.

An important advantage of the TPA technique is the possibility to perform measurements on scattering media. In contrast to depolarized dynamic light scattering experiments, scattering of the host complex does not significantly hamper the experiment or its interpretation, because the tracers are specifically labeled and therefore also specifically detected. Although the dynamic range of the anisotropy decay is affected by scattering, the time dependence of the anisotropy curve remains the same. The low tracer concentration typically needed for the experiments is exemplary for the sensitivity of the technique. In addition, a convenient feature of the organosilica tracer particles is that the dimensions and surface chemistry can be modified (between approximately 30 nm and 1 μm).[28] This opens possibilities to study not only the pore size distribution but also the local interactions between tracer spheres and complex media.

Acknowledgment. Gijsje Koenderink is thanked for fruitful discussions. Yehudi Levine is thanked for drawing our attention to the Voronoi construction. Marc van Zandvoort and Gijs van Ginkel are thanked for continuous support.

LA991603V